Pediatric Radiology (2024) 54:1497–1506
https://doi.org/10.1007/s00247-024-05977-7

ORIGINAL ARTICLE

Venous malformations in children: comparison between magnetic resonance imaging and histopathological findings

L. Tofanelli[1] · M. Napolitano[2] · V. Baraldini[3] · L. Moneghini[4]

Received: 24 September 2023 / Revised: 19 June 2024 / Accepted: 20 June 2024 / Published online: 4 July 2024

Abstract

Background Among low-flow vascular malformations, venous malformations are relatively frequent. The pathological patterns vary in severity and are generally characterized by dilated vessels and low-flow blood that over time can organize into phleboliths. Sometimes small capillary and/or lymphatic vessels may be associated, micro- and/or macro-shunts may form alone or in different combinations, and finally adipose tissue may be interposed between the malformed vessels. Magnetic resonance imaging (MRI) is a crucial examination for confirming venous malformations because it can accurately identify different features of the lesions.

Objective The aim of our study was to compare MRI and histopathological findings of venous malformations in children to assess the possibilities and limitations of MRI.

Materials and methods In a retrospective study, two observers independently evaluated the contrast-enhanced MRI of 26 children with venous malformations. Several radiological parameters were considered and compared with histopathological findings. The agreement between the interobserver radiological evaluation and between histopathological and radiological diagnosis was verified using Cohen's kappa.

Results MRI interobserver agreement was excellent for micro-shunts and good for the remaining findings. The radiological-pathological agreement was perfect for the presence/absence of phleboliths and of macro-shunts and almost perfect for the presence of intralesional adipose tissue, lymphatic component, and micro-shunts.

Conclusion MRI in venous malformations can detect the presence of phleboliths, adipose tissue, and lymphatic components with excellent accuracy and good to excellent interobserver agreement. Furthermore, MR angiography can detect micro-shunts in simple and combined venous malformations with substantial agreement with histopathological findings.

Keywords Histopathology · Magnetic resonance imaging · Pediatric · Venous malformation

Introduction

In 2018, the International Society for the Study of Vascular Anomalies (ISSVA) updated the classification for vascular anomalies, published in 2014 at the 20th ISSVA's seminar in Melbourne, Australia. In the ISSVA classification, vascular anomalies were divided into two groups: vascular tumors and vascular malformations [1]. Vascular malformations are generally congenital, differing from tumors by normal cell turnover and growth proportional to the patient's growth [2]. They are therefore subcategorized into simple malformations, when only one type of malformed vessel is present, and combined, when two or more simple vascular malformations are present in a single lesion.

By evaluating the characteristics of blood flow through the vessels, simple malformations can be divided into

✉ L. Moneghini
laura.moneghini@asst-santipaolocarlo.it

1 Department of Radiology, Santi Paolo e Carlo Hospital Medical School, University of Milan, Milan, Italy

2 Department of Pediatric Radiology and Neuroradiology, V. Buzzi Children's Hospital, Milan, Italy

3 Center for Pediatric Vascular Malformations-Pediatric Surgery Unit V. Buzzi Children's Hospital, Milan, Italy

4 Unit of Human Pathology, Department of Health Sciences, Santi Paolo e Carlo Hospital Medical School, University of Milan, Via Di Rudinì 8, 20148 Milan, Italy

high-flow (arteriovenous malformations and arteriovenous fistulae) and low-flow malformations (venous, capillary and lymphatic malformations) [1].

In a recent study published by ISSVA, soft tissue low-flow malformations are more common (1 per 1000 births) than high-flow malformations (1 case per 10,000 births) [3].

Among low-flow vascular malformations, venous malformations are relatively frequent, approximately 45 per 100,000, and lymphatic malformations are approximately 35 per 100,000 [3]. However, there is disagreement in the literature regarding the prevalence and incidence of vascular malformations in terms of subtype, as these are uncommon lesions [4].

Clinical and ultrasound evaluation are considered a first approach for the diagnosis of vascular malformations; however, MRI represents a crucial examination to better define their specific type, extension, and anatomic relationship to adjacent structures, providing important information for therapy planning [5]. It is recognized that after injection of contrast medium, the degree and type of filling of the venous channels in venous malformations varies [6, 7].

Some venous malformations are formed by veins that fill slightly earlier than adjacent veins from peripheral arterial branches and may be misinterpreted as high-flow malformations. In particular, based on time-resolved magnetic resonance angiography (MRA) performed at 3 tesla (T), a recent quantitative study considers venous malformations with arteriovenous micro-shunt and without arteriovenous micro-shunt as two distinct types of slow-flow vascular malformations. The authors analyzed only simple venous malformations and considered arteriovenous micro-shunts as small arteries directly connected to the venous malformations which lead to early enhancement of the lesion. They called this condition hypodynamic arteriovenous fistula to distinguish it from "hyperdynamic arteriovenous fistula" of high-flow malformations [7]. Previously, on angiography, Burrows et al. reported a similar contrast enhancement in some capillary-venous malformations [8]. However, this could be confusing because capillary-venous malformations are defined as malformations with combination of capillary and venous components while arteriovenous micro-shunts represent a different phenomenon. In fact, in low-flow combined malformations, small capillary and/or lymphatic vessels may be present in different combinations with venous malformations and adipose tissue can be present among the vessels [9].

The slow flow and blood stagnation in the distorted and enlarged vessels of venous malformations result in constant activation of coagulation named localized intravascular coagulopathy leading to the formation of thrombi and phleboliths. Localized intravascular coagulopathy is statistically associated with large and/or deep venous malformations that affect any location [10]. A retrospective study of 3T MR images reports arteriovenous micro-shunts in untreated venous malformations as a frequent phenomenon and significantly associated with phleboliths and large lesions [11]. All these hemodynamic changes resulting from the presence of arterial micro-shunts in venous malformations may require different management [7, 11].

Moreover, both previously mentioned studies focus on venous malformations with or without arteriovenous micro-shunt at 3T MRI, which lacks correlation with alternative invasive imaging and histopathologic findings.

The aim of the present study was to evaluate the characteristics of venous malformations, simple and combined, at the more accessible 1.5 T MRI, comparing them with histopathological findings to evaluate the possibilities and limitations of MRI.

Materials and methods

In a clinical audit from July 2007 to October 2019, 99 patients were investigated by histopathological examination with conclusive diagnosis of simple/combined venous malformation. Thirty-two patients had previously undergone MRA in our Institute; five patients were excluded due to significant movement artifacts and one because MRA was performed at a different site than biopsy. Histological examination was performed by L.M. (a pathologist of 15 years with expertise in vascular anomalies).

Magnetic resonance imaging protocol

Each patient was examined using a 1.5-T Achieva D-Stream (Philips, Best, the Netherlands), with dedicated surface coils (phased array head coil, knee coil, extremity coil, and body coil). All examination protocols included sequences for morphologic characterization based on a localizer sequence, axial unenhanced T1-weighted turbo-spin-echo (TSE), axial and coronal (or sagittal) T2-weighted TSE, axial and coronal (or sagittal) short-tau inversion recovery (STIR) acquisition, or T2-weighted fat-saturated sequences and sequences for hemodynamic characterization during contrast medium injection: T1-weighted high-resolution three-dimensional (D) time-resolved angiography (FFE) time-resolved angiography (4-D/HR) in coronal or sagittal plane and an T1-weighted high resolution 3-D gradient echo with fat suppression (THRIVE) or an axial 3-D T1-weighted modified Dixon or an axial fat suppressed T1-weighted sequence 5–8 min after gadolinium injection.

Two types of gadolinium-based contrast were used: gadoteric acid (0.2 ml/kg, Dotarem; Guerbet, Villepinte, France) or Gadobutrol (0.1 ml/kg, administered intravenously; Gadovist; Bayer B.V., Leverkusen, Germany). We excluded the MRI exam if some of these sequences were missing or if the examination was not optimal (movement artifacts). In our protocol, 4-D/HR was used as time-resolved MRA

technique with a contrast enhancement profile "centra" (contrast-enhanced timing robust angiography) and a Cartesian acquisition mode. It had thin slices (1.5 mm), very short TR (5.2) and TE (1.45), and flip angles of 35–40°. The initial image without contrast was used as a mask for subtraction to improve vascular visibility. Data of the different partial k-space samplings were combined to create a series of time-resolved images with an adequate spatial resolution (size of acquired pixel was usually 0.72 × 1.42 mm; reconstructed pixel size was 0.63Å ~ 0.63 mm). Dynamic sequences were started 10 s before contrast medium injection, to generate at least one dataset without contrast medium. In our study, high temporal resolution ranges from 3–14 s.

Magnetic resonance imaging features

MRIs were evaluated independently by two radiologists (L.T. and M.N. with 25 years and 5 years of experience respectively), blinded to histopathological findings for the presence/absence of phleboliths, micro-shunt, and lymphatic and adipose components. In addition, size, volume (using the formula: height × width × length × 1/6 π), lesion location (subcutaneous, muscle, and bone tissue), and appearance (localized or diffuse angioarchitecture) were considered (Table 1). The phleboliths were recognizable as round foci of hypointensity in all MRI sequences and were differentiable from thrombi, usually hyperintense in T1, and from muscle fibers characterized by more elongated morphology [12–14]. The presence of adipose tissue was evaluated by comparing the morphological sequences with and without adipose tissue suppression. Due to possible estimation errors, the adipose component was not evaluated in the predominantly subcutaneous lesion. Lymphatic components usually appear as iso-hypointense in T1 sequences and hyperintense in T2-weighted images, and the use of gadolinium facilitates the differentiation between venous malformations and lymphatic malformations because gadolinium only accumulates in venous malformations [11]. Indeed, although lymphatic malformations may show a slight late increase in septa, they are not composed of blood vessels. Therefore, the lymphatic component in the venous malformations was evaluated using morphological sequences and T1-TSE weighted after gadolinium injection. Dynamic sequences were required to distinguish the type of malformation and the presence of arteriovenous micro-shunts was detected by the early and progressive potentiation of venous malformations, provided by the dilated arterial vessels, before any opacification of the veins. In venous malformations without micro-shunt, the arterial branches feeding the malformation were not visible, so when the lesion increased contrast, the drainage veins were already opaque [7].

Histological examination

Twenty-two (85%) samples were composed of soft tissue and skeletal muscle tissue obtained from surgical excision of symptomatic lesions, and four (15%) samples were obtained from diagnostic biopsy. Samples were fixed in formalin for histological and immunohistochemical evaluation. Sampling and staining of each case were performed according to the study by Moneghini et al. [15]. For each case, different histological parameters were evaluated: luminal blood thrombi were considered blood clots at different stages of organization up to the formation of phleboliths in which the calcification was histologically evident with hematoxylin/eosin staining or with the use Von Kossa stain to detect calcium deposits.

The lymphatic component was easily identified with the positivity of immunohistochemical staining for podoplanin (clone D2-40) in endothelial cells, while the micro-shunts were recognizable as medium-/small-caliber veins with duplication of elastic fibers in the wall, as an effect of high pressure that the vessel had undergone, also known as "arterialization" of the vascular wall [9]. Histochemical

Table 1 Features evaluated and sequences used on magnetic resonance imaging

Sequences	Evaluated features
Axial and coronal (or sagittal) STIR or T2-weighted fat-saturated	Size of the lesion and appearance
STIR or T2-weighted fat-saturated or T2-weighted; unenhanced axial T1-weighted sequence and axial T1-weighted fat-saturated after gadolinium enhancement	Presence of phleboliths
Comparison between unenhanced axial T1-weighted and axial T1-weighthed fat-saturated and/or comparison between T2-weighted TSE and STIR or T2-weighted fat-saturated	Presence of fat
Axial STIR or T2-weighted fat-saturated and T1-weighted sequence	Localization (muscle, subcutis, bone)
Time-resolved MRA techniques	Flow dynamics: vascular supply, venous system, presence/absence of micro-shunts and macro-shunts
STIR or T2-weighted fat-saturated and Axial T1-weighted fat-saturated after gadolinium enhancement	Lymphatic component

MRA magnetic resonance angiography, *STIR* short tau inversion recovery, *TSE* turbo spin echo

Orcein staining was also used to better recognize "arterialization" aspects. Vessel density in the venous malformations was variable, and the tissue interposed between the vessels consisted of tissue from the involved organ, such as mainly muscle fiber bundles in skeletal muscle tissue and connective tissue and/or adipose tissue in soft tissue. Adipose tissue may be particularly abundant in some cases of venous malformations, both in skeletal muscle and soft tissue [16].

Cohen's kappa (K) was used to statistically assess the agreement between MRI and histopathological findings and for interobserver agreement between the two radiologists (Table 2). Accuracy, sensitivity, specificity, and positive and negative predictive value were also determined. Cohen's K can vary between 0 and 1: values ≤ 0 indicating no agreement, 0.01–0.20 none to poor, 0.21–0.40 fair, 0.41–0.60 moderate, 0.61–0.80 substantial, and 0.81–1.00 nearly perfect agreement.

Where the radiologists reported different findings in MRI examinations, these were discussed between them and agreement reached for comparison with pathological anatomy. Subsequently, histopathology and MRI features were

Table 2 Agreement between magnetic resonance imaging and pathological anatomy and interobserver agreement between two radiologists on magnetic resonance imaging

Magnetic resonance imaging versus histopathologic findings (26 patients)								
Features	Phleboliths (26 patients)		Micro-shunts (26 patients)		Adipose Component[a] (21 patients)		Lymphatic Component (26 patients)	
	Absent on histopathological analysis	Present on histopathological analysis	Absent on histopathological analysis	Present on histopathological analysis	Absent on histopathological analysis	Present on histopathological analysis	Absent on histopathological analysis	Present on histopathological analysis
Absent on magnetic resonance imaging	17	0	15	1	12	2	19	2
Present on magnetic resonance imaging	0	9	2	8	0	7	0	5
Cohen's K	1		0.752		0.800		0.785	
Sensitivity	100%		89%		78%		71%	
Specificity	100%		88%		100%		100%	
Accuracy	100%		88%		90%		92%	
PPV	100%		80%		100%		100%	
NPV	100%		94%		86%		90%	
Interobserver agreement on magnetic resonance imaging (26 patients)								
Features	Phleboliths (26 patients)		Micro-shunts (26 patients)		Adipose Component[a] (21 patients)		Lymphatic Component (26 patients)	
	Not detected by the radiologist A	Detected by the radiologist A	Not detected by the radiologist A	Detected by the radiologist A	Not detected by the radiologist A	Detected by the radiologist A	Not detected by the radiologist A	Detected by the radiologist A
Not detected by the radiologist B	17	0	15	1	14	0	21	0
Detected by the radiologist B	0	9	1	9	0	7	0	5
Cohen's k	1		0.837		1		1	
Agreement	100%		92%		100%		100%	

The first section of the table shows the agreement between magnetic resonance imaging and pathological anatomy

[a]Only 21 of the 26 patients were evaluated for the adipose component: five patients were excluded because adipose components were not adequately assessable on magnetic resonance imaging

The second section of the table shows the interobserver agreement on magnetic resonance imaging

Radiologist A has over 20 years of experience in pediatric radiology and vascular malformations, while radiologist B has approximately 5 years of experience

associated separately with the type of malformation or with each using the chi-square test. *P* value 0.05 was considered significant.

Results

A total of 26 (12 boys) patients aged under 18 years (median 8 years), with venous malformations at different localizations were included in this retrospective study: face-neck (*n*=8), upper limb (*n*=7), and lower limb (*n*=11). Fifteen venous malformations (58%) were localized while the remaining eleven (42%) were diffuse. Subcutaneous tissue or skeletal muscle was involved by venous malformations in 34.5% (9/26) of cases; in 27% (7/26) of cases, both muscle and subcutaneous tissue were involved, while only one venous malformation (4%) involved bone, skeletal muscle, and subcutaneous tissue. The median volume of the lesion was 11 ml (interquartile range 4–68 ml). MRI interobserver agreement was 100% (K=1) for the different features (presence/absence of phleboliths, lymphatic and adipose components) with only minimal disagreement concerning the identification of arteriovenous micro-shunts, while still maintaining a high level of agreement (K=0.837; 92% agreement) (Table 2).

Histologically, 15/26 were diagnosed as simple venous malformations and the remaining 11 as combined: 3/26 capillary-venous malformations, 3/26 capillary-lymphatic-venous malformations, and 4/26 lymphatic-venous malformations while one venous malformation with arterovenous macro-shunt developed after a traumatic event.

Nine (33%) malformations presented histologically arteriovenous micro-shunts (Fig. 1): four were simple venous malformations, two capillary-venous malformations, and the remaining three were respectively a capillary-lymphatic-venous malformation, a lymphatic-venous malformation, and the malformation with arteriovenous macro-shunt.

All lesions that were described histologically as simple or combined venous malformations were classified on MRI as low-flow vascular malformations; both radiologists correctly identified the one exception with macro-shunt.

Considering histopathology as the gold standard, the diagnostic accuracy of MRI was 100% in the detection of phleboliths and 92% and 90% in that of lymphatic and adipose components, respectively, while slightly lower (88%) for arteriovenous micro-shunts (Table 2).

On MRI, more specifically, there was one false negative and two false positives for the detection of arteriovenous

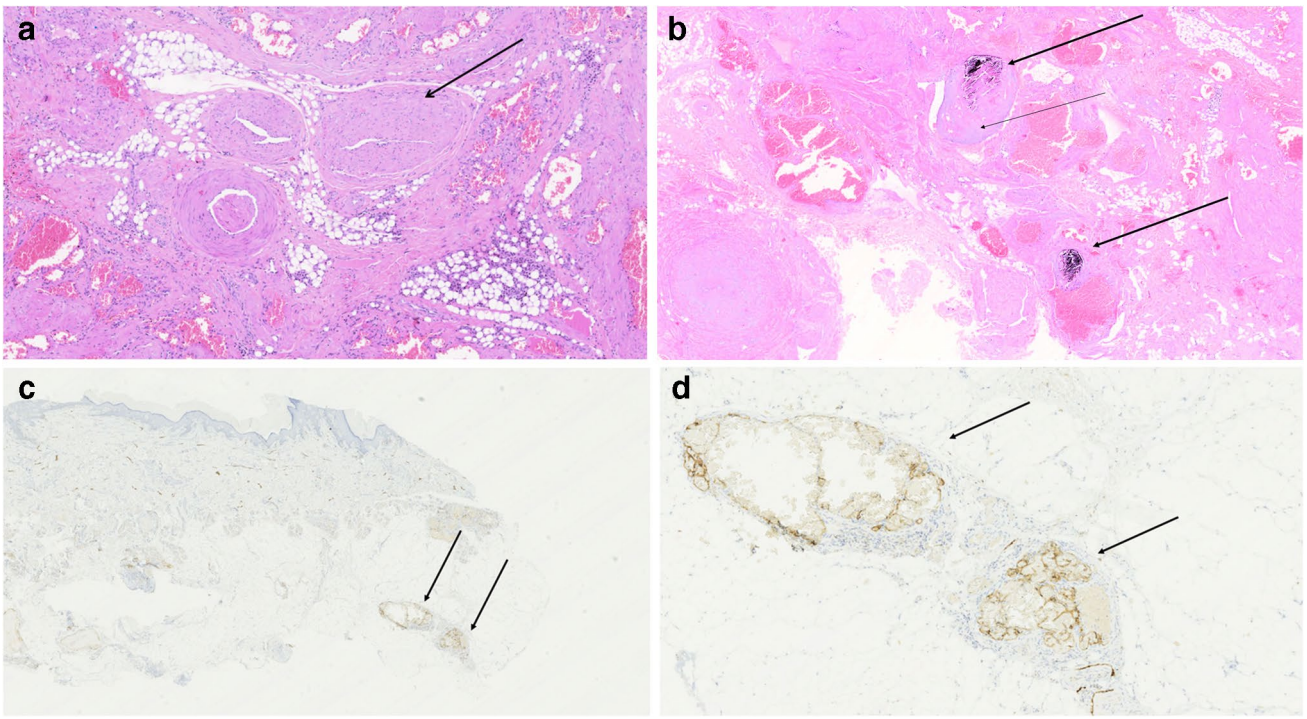

Fig. 1 **a**, **b** Histopathology slides using hematoxylin and eosin stain and shown at 4×magnification in a 6-year-old girl with soft tissue and intramuscular venous malformation of the lower limbs. **a** A venous malformation with arteriovenous micro-shunts (*arrow*) and fat tissue interposition in soft tissue. **b** Shows a venous malformation with phlebolith formation (*thick arrows*) in thrombotic vessels (*thin arrow*) in the soft tissues. **c**, **d** Histopathology slides using D2-40 stain at 4×(**c**) and 10×(**d**) magnification in an 8-year-old girl with a soft tissue capillary-lymphatic-venous malformation of the face and neck. Note the lymphatic micro-component in the hypodermis (*arrows*) (4×, D2-40)

micro-shunts (K=0.752, accuracy 88%). In our study, the presence of arteriovenous micro-shunts was not significantly associated with phleboliths (P=0.920) or lymphatic components (P=0.694), while there was a statistically significant correlation with localized angioarchitecture (P=0.019). An example of venous malformations with arteriovenous micro-shunts on MRI is shown in Fig. 2.

Discussion

Our study shows that MRI has an excellent diagnostic accuracy for low-flow vascular malformations such as venous malformations, simple or combined, even considering the interobserver variability. MRI can detect the presence of phleboliths in venous malformations with an excellent accuracy and similarly for lymphatic vessels (Fig. 3) and adipose tissue and has a high positive predictive value (PPV in Table 2). However, small components such as scattered adipocytes or small lymphatic vessels may not be detected, possibly due to the inherent limitations of MRI (Fig. 1 and Fig. 4). Furthermore, the lymphatic component, in particular micro-cystic lesions, may have mild increase in contrast and therefore could be confused with a part of the malformation. Alternatively, more intense venous malformation enhancement could obscure the lymphatic component.

In our study as previously described, small hemodynamically irrelevant arteriovenous micro-shunts in venous malformations led to early lesion enhancement (Fig. 2). Differing from Hammer et al., we did not analyze only simple venous malformations and, at histopathology, we detected arteriovenous micro-shunts and combined venous malformations such as capillary-venous malformation, capillary-lymphatic-venous malformation, lymphatic-venous malformation, and complicated venous malformation with arteriovenous macro-shunt. Therefore, arteriovenous micro-shunts can even be found in the presence of vascular malformations with capillaries and lymphatic vessels. In effect, as abovementioned, Burrows et al. described this type of enhancement in capillary-venous malformations on angiographs. However, venous malformations with arteriovenous micro-shunts and capillary-venous malformations are distinct concepts: arteriovenous micro-shunts are visible as arterialized veins of medium caliber (i.e. veins with

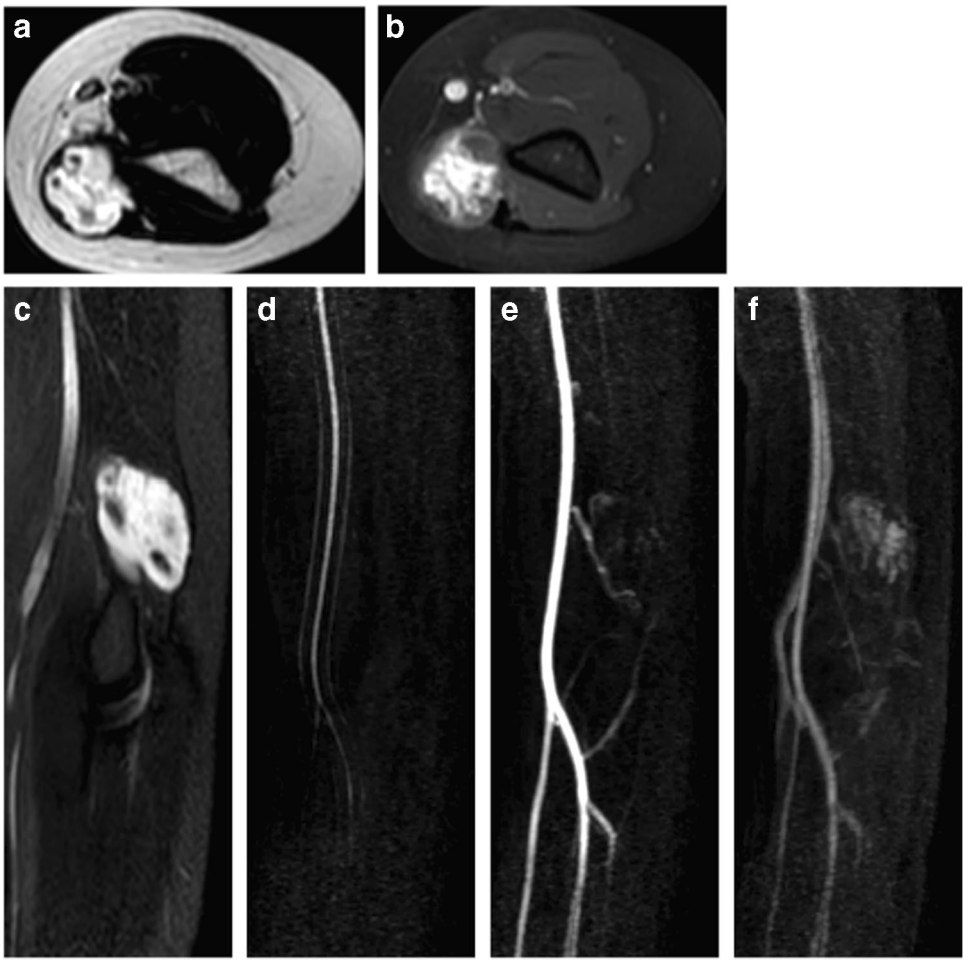

Fig. 2 Magnetic resonance images of a localized, intramuscular venous malformation of the left arm with arteriovenous micro-shunts in a 6-year-old girl. **a** Axial T2-weighted turbo-spin-echo image shows hyperintensity and phleboliths. **b** Axial fat saturated contrast-enhanced T1-weighted turbo-spin-echo image shows diffuse contrast-enhancement of venous malformation. **c** Coronal short tau inversion recovery image shows phleboliths. **d**–**f** Corresponding coronal maximum-intensity-projection time resolved magnetic resonance angiography images at 0 (**d**), 5 (**e**), and 40 s (**f**) after onset of arterial enhancement. Lesion enhancement began 5 s after arterial enhancement showing arteriovenous micro-shunts (**e**)

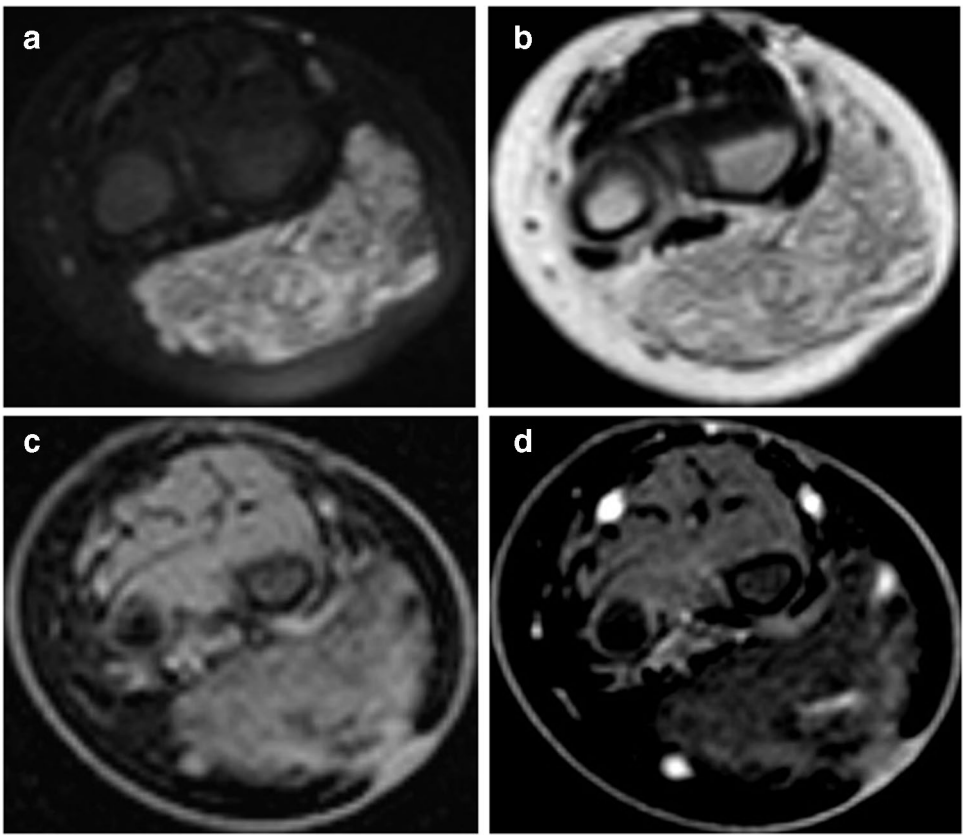

Fig. 3 Axial magnetic resonance images of a lymphatic-venous malformation with predominant lymphatic component without arteriovenous micro-shunts in the forearm of a 2-year-old boy. **a** Axial T2-weighted turbo-spin-echo with fat saturation image shows typical hyperintense signal of the lymphatic-venous malformation. **b** Axial T2-weighted turbo-spin-echo image shows the high-to-intermediate signal lesion. **c** Axial unenhanced T1-weighted high-resolution isotropic volume examination (*THRIVE*) image shows an isointense lesion. **d** Corresponding axial T1-weighted contrast-enhanced *THRIVE*, 6 min after gadolinium injection, showing a poor enhanced lesion: there is a prevalent component with absent enhancement and a peripheral component with minimal enhancement probably due to minimal venous component interposed

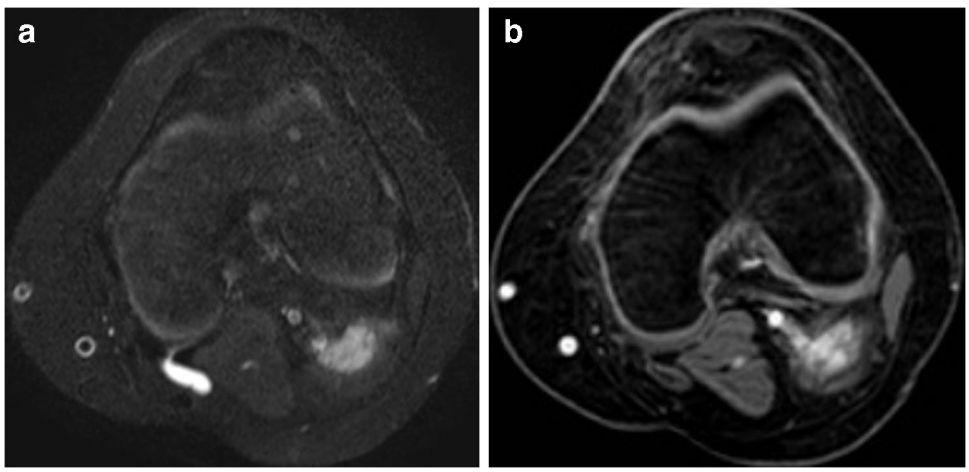

Fig. 4 Axial magnetic resonance images of an intramuscular capillary-lymphatic-venous malformation of the right leg with arteriovenous micro-shunts in a 1-year-old girl. **a** Axial T2-weighted turbo-spin-echo with fat saturation image shows the hyperintense signal of the capillary-lymphatic-venous malformation. **b** Corresponding axial post-contrast T1-weighted high-resolution isotropic volume examination image shows a well-circumscribed enhancing lesion with a lymphatic component not clearly visible

duplication of elastic fibers) (Fig. 1), while capillary-venous malformations are defined as a venous malformations associated with a capillary component [6]. In fact, in our experience one patient with capillary-venous malformation and two with capillary-lymphatic-venous-malformations did not have arteriovenous micro-shunts on histological examination nor were these considered to be present on MRI. In a combined malformation, we assume that the capillary component is difficult to detect on MRI, especially when the vascular malformation is intramuscular.

Similar to Hammer et al., we observe that the presence of arteriovenous micro-shunts in venous malformations is a frequent phenomenon. Hammer et al. supported the hypothesis that arteriovenous micro-shunts were the result of thrombosis in malformed vessels because the number of phleboliths was significantly increased in venous malformations with arteriovenous micro-shunts [11]. In contrast to this finding, the history of thrombophlebitis was not significantly increased in the subgroup of venous malformations with arteriovenous micro-shunts, and in our study, we did not observe a significant association between arteriovenous micro-shunts and phleboliths, perhaps because we did not analyze only simple venous malformations.

Perhaps faster blood flow in these low-flow lesions reduces the frequency of thrombophlebitis, due to a "flushing effect" [7]. Furthermore, arteriovenous micro-shunts were mainly present in localized lesions (Fig. 2) compared to diffuse malformations, in contrast to another study in which there was no correlation with angio-architecture [11]. Using a 3T scanner, Hammer et al. reported a significant difference in "t onset" (interval between the onset of arterial enhancement in an adjacent artery and lesion enhancement) between venous malformations with and without arteriovenous micro-shunts [7].

In our study, the time resolution of the MRA exam had a wide distribution range (3–14s) because over the years, although the MR-scanner was the same, the software updates have allowed a higher compressed sense and therefore a faster parallel imaging. The time was also different in relation to the acquisition volume and to the extension of the venous malformations. For the wide distribution range, we could not accurately establish the difference in t onset (time interval between onset of enhancement in an adjacent artery and within the lesion) between the venous malformations with and without arteriovenous micro-shunts. However, the group with arteriovenous micro-shunts had a shorter average t onset compared to the group without arteriovenous micro-shunts, though the only false negative in MRA, it had a late enhancement (at about 16 s). In addition, the two false positive cases at MRA had an early "t onset": 8 s and 11 s, respectively. The first case could be related to the paucity of the sample for the histopathological examination. Perhaps the lesion had an arteriovenous micro-shunt in a different region of the sample. In the second case, since the range of acquisition was wide, the enhancement was interpreted as early, even though it most likely was not. For this reason, also considering the median t onset in the study of Hammer et al. and to better distinguish high-flow lesions, it is preferable to set a high temporal resolution for MRA of 5.0–5.5 s [7]. Sequence parameters and a standard protocol are shown for non-dynamic and dynamic sequences in Tables 3 and 4, respectively.

The major limitation of the present study is its retrospective design with a relatively wide range of temporal resolution in a non-standardized MRA protocol and by the lack of quantitative criteria for evaluation of time-resolved MRA. Moreover, it was not possible to correlate these data with preoperative color-Doppler scan or clinical findings.

Other limitations are the small study cohort and the possible errors resulting from comparison with just a sample of malformations [17].

In addition, there may have been changes in venous malformations from the time of MRI to the time of tissue sampling for histopathological examination.

We propose a diagnostic MRI pathway (Fig. 5) which may be useful in the evaluation of vascular malformations. However, some benign and malignant soft tissue lesions can

Table 3 Parameters of morphological and post-contrast injection sequences

Morphological and post-contrast injection sequences				
Parameter	STIR	STIR	Axial TSE-T2	3-D T1 modified Dixon axial before and post (5 min) gadolinium injection
Orientation	Coronal	Axial	Axial	Axial
TR/TI (ms)	3782/150	4881/50	3603	5.4
TE (ms)	50	50	100	3.7
TSE/TFE factor	23	27	21	15
Flip angle (°)	NA	NA	90	10
ACQ voxel size (mm × mm × mm)	1.10×1.11×4.00	1.19×1.29×5.00	1.14×1.3×6.00	1.5×1.5×3.00
REC voxel size (mm × mm × mm)	0.78/0.78/4.00	0.78/0.78/5.00	0.78/0.78/5.00	0.45×0.45×0.45

Non-dynamic sequences (morphological and post-contrast) and respective parameters for the study of vascular malformations on magnetic resonance. This is a standard protocol; it must be adapted according to the region of interest

ACQ acquired, *D* dimensional, *REC* reconstructed, *STIR* short tau inversion recovery, *TE* echo time, *TFE* turbo field echo, *TI* inversion time, *TR* repetition time, *TSE* turbo spin echo

Table 4 Standard sequence parameters of time-resolved magnetic resonance angiography. These sequences must be adapted based on the region of interest

	Time-resolved magnetic resonance angiography (3-D FFE T1)
Orientation	Coronal
TR/TI (ms)	5.2
TE (ms)	1.43
Flip angle (°)	40
Time to K0 (s)	2
Dynamic scan time (s)	5.4
Acquisition mode	Cartesian
Technique of acceleration	CS-SENSE
Acceleration factor	5
Number of time frames	16
ACQ voxel size (mm × mm × mm)	0.72×1.43×3.5
REC voxel size (mm × mm × mm)	0.63×0.63×1.75

ACQ acquired, *CS-SENSE* compressed sensing-sensitivity encoding, *D* dimensional, *FFE* fast field echo, *TE* echo time, *TI* inversion time, *TR* repetition time, REC reconstructed

mimic vascular malformations both clinically and on imaging; for this reason, it is essential to integrate the medical history, clinical data, and ultrasound examination to arrive at a correct diagnosis.

In summary, MRI is known to be the mainstay of imaging for vascular malformations. MRI represents the best method to characterize simple or combined venous malformations, also detecting the presence of intralesional adipose and lymphatic components; however, if small in number/volume, the individual components may not be technically detectable. Venous malformations with arteriovenous micro-shunts are distinct from those with a capillary component and can be identified in MRI as early enhancement of the lesion without immediate venous outflow. This distinction is important because venous malformations with arteriovenous micro-shunts might have a different response to sclerotherapy treatment.

In effect, higher blood flow within the venous malformation could wash away the injected sclerosing agent. Further studies are needed to investigate whether venous malformations with arteriovenous micro-shunts require different management to venous malformations without arteriovenous

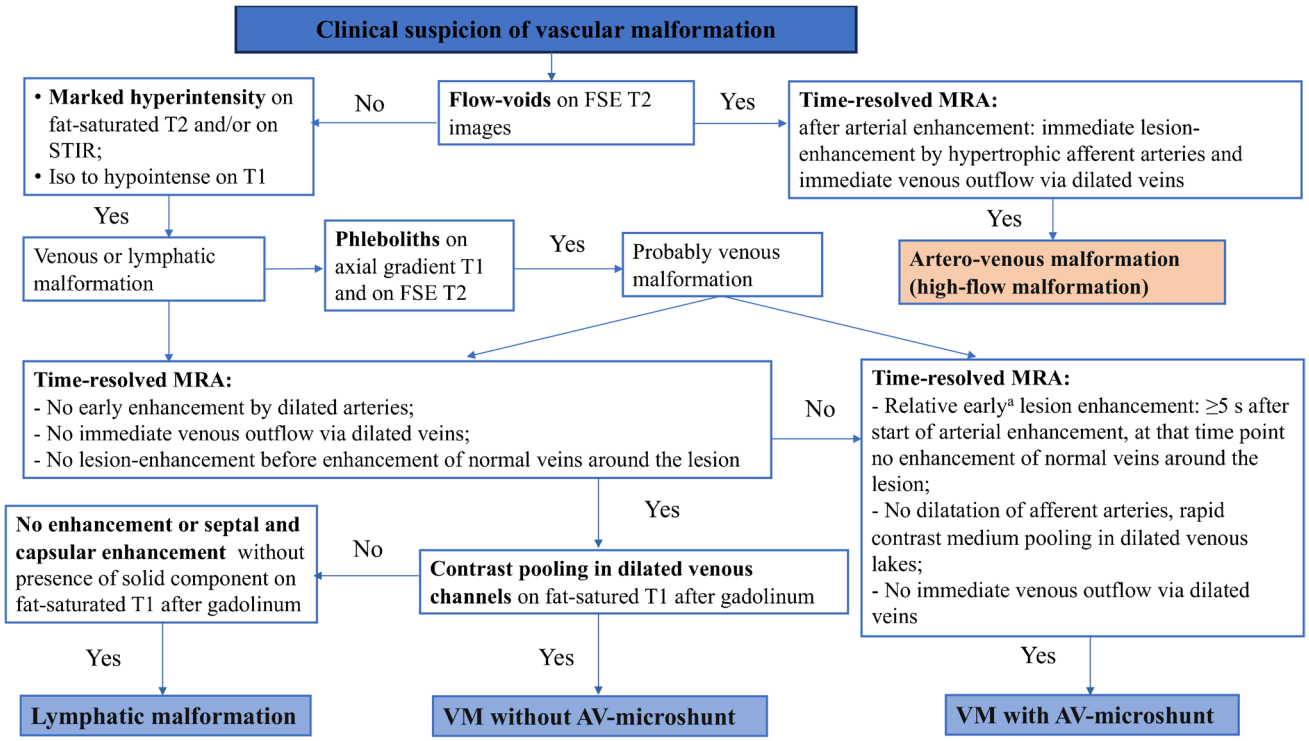

Fig. 5 Proposed diagnostic flowchart for vascular malformations on magnetic resonance imaging. It is essential to consider clinical-anamnestic data for a proper diagnosis and radiologists should be aware that some lesions on magnetic resonance imaging can mimic vascular malformations [13, 15]; as reported by Hammer et al., relative early enhancement is not immediate, as in high-flow lesion in which enhancement of the lesion is immediate after arterial enhancement of the main artery in the region of interest with immediate venous outflow via dilated veins, but ≥ 5 s after arterial enhancement in the region without any enhancement of normal veins around the lesion [7]. *AV* arteriovenous, *FSE* fast spin echo, *MRA* magnetic resonance angiography, *STIR* short tau inversion recovery, *VM* venous malformation

micro-shunts. Moreover, the presence of arteriovenous micro-shunts within venous malformations may indicate a particular subtype of venous malformation, which requires further investigation to characterize its genetic etiology.

Conclusion

This study demonstrates that MRI has excellent diagnostic accuracy in diagnosing low-flow vascular malformations such as venous malformations, simple or combined, both compared with the corresponding histological findings and considering interobserver variability. Arteriovenous micro-shunts in untreated simple venous malformations are a frequent phenomenon but can also be found in combined venous malformations.

The diagnostic accuracy of MRI in identifying the different components of venous malformations can further contribute to the choice of treatment to be adopted.

Acknowledgements We would like to thank M.D.A. Zocca for writing assistance, Mr. M. Vallinoti for computer support and Mr. G. Di Leo for statistical analysis.

Author contribution L.T. and L. M. conceived the study; M. N. and L. T. performed imaging studies; V. B. supported clinical data; L. M. performed histological analysis.

Data availability The imaging datasets generated, analyzed, and presented during the current study are available from the corresponding author upon request.

Declarations

Conflicts of interest None

References

1. ISSVA Classification of vascular anomalies ©2018 International Society for the Study of Vascular Anomalies Available at "issva.org/classification" Accessed March 2024
2. Kunimoto K, Yamamoto Y, Jinnin M (2022) ISSVA Classification of vascular anomalies and molecular biology. Int J Mol. https://doi.org/10.3390/ijms23042358
3. Penington A, Phillips RJ, Sleebs N, Halliday J (2023) Estimate of the prevalence of vascular malformations. J Vasc Anomalies. https://doi.org/10.1097/jova.0000000000000068
4. Ryu JY, Chang YJ, Lee JS et al (2023) A nationwide cohort study on incidence and mortality associated with extracranial vascular malformations. Sci Rep. https://doi.org/10.1038/s41598-023-41278-z
5. Flors L, Leiva-Salinas C, Maged IM et al (2011) MR imaging of soft-tissue vascular malformations: diagnosis, classification, and therapy follow-up. Radiographics. https://doi.org/10.1148/rg.315105213
6. Legiehn GM, Heran MKS (2006) Classification, diagnosis, and interventional radiologic management of vascular malformations. Orthop Clin North Am. https://doi.org/10.1016/j.ocl.2006.04.005
7. Hammer S, Uller W, Manger F et al (2017) Time-resolved magnetic resonance angiography (MRA) at 3.0 Tesla for evaluation of hemodynamic characteristics of vascular malformations: description of distinct subgroups. Eur Radiol. https://doi.org/10.1007/s00330-016-4270-1
8. Burrows PE, Mulliken JB, Fellows KE, Strand RD (1983) Childhood hemangiomas and vascular malformations: angiographic differentiation. Am J Roentgenol. https://doi.org/10.2214/ajr.141.3.483
9. North PE (2010) Pediatric vascular tumors and malformations. Surg Pathol Clin. https://doi.org/10.1016/j.path.2010.07.002
10. Hung JWS, Leung MWY, Liu CSW et al (2017) Venous malformation and localized intravascular coagulopathy in children. Eur J Pediatr Surg. https://doi.org/10.1055/s-0036-1582241
11. Hammer S, Zeman F, Fellner C et al (2018) Venous malformations: phleboliths correlate with the presence of arteriovenous microshunts. Vascular and Interventional Radiology. https://doi.org/10.2214/AJR.18.19703
12. Merrow AC, Gupta A, Patel MN, Adams DM (2016) 2014 revised classification of vascular lesions from the international society for the study of vascular anomalies: radiologic-pathologic update. Radiographics 36:1494–1516
13. Olivieri B, White CL, Restrepo R et al (2016) Low-flow vascular malformation pitfalls: from clinical examination to practical imaging evaluation - part 2, venous malformation mimickers. Am J Roentgenol. https://doi.org/10.2214/AJR.15.15794
14. Restrepo R (2013) Multimodality imaging of vascular anomalies. Pediatr Radiol. https://doi.org/10.1007/s00247-012-2584-y
15. White CL, Olivieri B, Restrepo R et al (2016) Low-flow vascular malformation pitfalls: from clinical examination to practical imaging evaluation - part 1, lymphatic malformation mimickers. Am J Roentgenol. https://doi.org/10.2214/AJR.15.15793
16. Moneghini L, Mihm MC, Fulcheri E (2019) Procedures and operating instructions for diagnosis in vascular anomalies and pathology. Pathologica. https://doi.org/10.32074/1591-951X16-19
17. van Rijswijk CSP, van der Linden E, van der Woude H et al (2002) Value of dynamic contrast-enhanced MR imaging in peripheral vascular malformations. AJR Am J Roentgenol. https://doi.org/10.2214/ajr.178.5.1781181